LAGRANGIAN FLOW GEOMETRY OF TRIPOLAR VORTEX

Lorena A. Barba[1] and Oscar U. Velasco Fuentes[2]

[1] Department of Mathematics, University of Bristol, UK
l.a.barba@bristol.ac.uk
[2] Depto. de Oceanografía Física, CICESE, Ensenada, México
ovelasco@cicese.mx

Abstract. Tripolar vortices have been observed to emerge in two-dimensional flows from the evolution of *unstable* shielded monopoles. They have also been obtained from a *stable* Gaussian vortex with a large quadrupolar perturbation. In this case, if the amplitude of the perturbation is small, the flow evolves into a circular monopolar vortex, but if it is large enough a stable tripolar vortex emerges. This change in final state has been previously explained by invoking a change of topology in the co-rotating stream function. We find that this explanation is insufficient, since for all perturbation amplitudes, large or small, the co-rotating stream function has the same topology; namely, three stagnation points of centre type and two stagnation points of saddle type. In fact, this topology lasts until late in the flow evolution. However, the time-dependent Lagrangian description can distinguish between the two evolutions, as only when a stable tripole arises the hyperbolic character of the saddle points manifests persistently in the particle dynamics (i.e. a hyperbolic trajectory exists for the whole flow evolution).

Keywords: Lagrangian flow, tripolar vortex, scatter plot

1. Introduction

The tripole is a two-dimensional flow structure consisting of a linear arrangement of three vortices, of alternating sign. The whole structure rotates in the direction of the core vortex rotation. It has been observed in the laboratory in rotating [14, 15] and stratified fluid [7], where it is the product of growth and saturation of the instability of a shielded (zero net circulation) monopolar vortex. Tripole generation from unstable monopoles has also been addressed in numerical studies [4, 11]. More recently, the tripolar vortex was observed to emerge from the destabilization of a Gaussian monopole by a strong quadrupolar perturbation [13]. In this case, the structure does not have total circulation equal to zero ("shielded" case), but rather can have satellites of varying strength, in relation to the core vortex. The amplitude of the quadrupolar component in the initial condition determines whether

A.V. Borisov et al. (eds.), IUTAM Symposium on Hamiltonian Dynamics, Vortex Structures, Turbulence, 247–256.

the flow will evolve into a monopole or a tripole, and the existence of a critical amplitude was conjectured [13].

A systematic parameter study with the goal of determining the critical amplitude separating the monopole and tripole as asymptotic states is presented in [1]. There, the authors performed dozens of simulations at different Reynolds numbers and perturbation amplitudes, and isolated a threshold leading to the tripole. The relaxation timescale was also investigated, as well as the stability properties of the tripolar structure and the evolution of the azimuthal modes. Here, we take an alternative approach to investigate the conditions leading to the persistence of the negative inclusions as satellite vortices, or their straining and mixing, leading to axisymmetrization. For various combinations of parameters, we analyze the essentially time-dependent Lagrangian flow geometry of the vortex, that is, the set of hyperbolic trajectories of the velocity field and their stable and unstable manifolds.

The problem of the perturbed Gaussian vortex is set up by calculating the relaxation of an initial condition consisting of the following vorticity field:

$$\omega(\mathbf{x}) = \frac{1}{4\pi} \exp\left(\frac{-|\mathbf{x}|^2}{4}\right) + \frac{\delta}{4\pi} |\mathbf{x}|^2 \exp\left(\frac{-|\mathbf{x}|^2}{4}\right) \cos(2\theta). \tag{1}$$

The first term on the right-hand side of (1) corresponds to the normally stable Gaussian vortex; the second term is a quadrupolar perturbation characterized by its amplitude, δ. In [13], three values of $\delta = 0.02,\ 0.1,\ 0.25$ were used for a Reynolds number $Re = \Gamma/\nu = 10^4$, where $\Gamma = 1$ is the circulation of the base vortex. It was found that for the larger amplitude value used, $\delta = 0.25$, the flow does not relax to an axisymmetric state, but rather develops into a quasi-steady, rotating tripole. This result was remarkable for two reasons: it contradicted the prevailing assumption that non-axisymmetric perturbations to a stable monopole would decay and axisymmetrize; and, it showed that the tripole could be generated other than as a result of the instability of shielded monopoles. The authors of [13] suggested that for large amplitudes the negative part of the initial perturbation resists mixing, and forms the satellites of the tripole, due to the creation of a *separatrix* in the streamline pattern observed in a reference system that co-rotates with the vortex structure.

The geometry of the co-rotating streamfunction is commonly used to explain diverse processes in two-dimensional vortex dynamics. It was used to explain vortex axisymmetrization in [9], and vortex merger in [5, 10] and other works. However, it has been pointed out that there is a flaw in this approach when it is applied to flows which are inherently time dependent [16,17]. One needs to compute the Eulerian flow geometry in a reference frame chosen so that the flow appears to be stationary, but this can only be done for flows which translate or rotate steadily. In truly time-dependent flows there are no co-moving frames, and the best one can do is find a frame where the flow is approximately stationary. This can be done by different methods, the choice of which is arbitrary; e.g., one method consists in approximating stream contours

by ellipses, and then observing the angular change of the main axis of the ellipse over time [10]; a second method is based on calculating second moments of vorticity [13]; a third method minimizes a quantity which measures how closely contours or ω and ψ are matched [6]. The important point to remember is that there is *not* a unique frame which co-rotates with a time-dependent vortex structure.

A more appropriate analytical technique for the study of unsteady velocity fields is the Lagrangian flow geometry. By looking at the hyperbolic trajectories and their stable and unstable manifolds, calculated from the numerically generated time evolving velocity fields, we make several observations regarding the tripole. We also note that the Lagrangian and Eulerian flow geometries differ appreciably, and thus it is not correct to ascribe the permanence of the satellites to the formation of a "critical separatrix", as argued previously [13]. In fact, the separatrices are present at the initial time, even in cases where the flow axisymmetrizes. How close the flow is to steady-state is assessed using scatter plots of vorticity versus stream function, as shown in Fig. 2. As a quasi-steady tripole is approached, the Lagrangian and Eulerian geometries are more alike, as in the last frame of Figs. 4(a) and 4(b). Additional observations for various cases will be presented below, but first we describe in §2. the numerical methods used.

2. Numerical methods

2.1. The vortex method

The time evolution of flow fields described in this work was computed with a vortex method especially adequate for high-Reynolds number flows [2]. The method is completely grid-free and is characterized by very low numerical diffusion and freedom from stability constraints in the choice of a time step (i.e., there is no equivalent to the Courant–Friedrichs–Lewy condition on this method). We begin by establishing an initial vorticity field, which evolves governed by the vorticity transport equation:

$$\frac{\partial \omega}{\partial t} + \mathbf{u} \cdot \nabla \omega = \nu \Delta \omega. \tag{2}$$

The evolution equation is solved by discretizing the vorticity field into disconnected elements, or particles of vorticity, each one represented by a position vector and a local distribution of vorticity. The discretized vorticity field is obtained from the sum of all particle contributions,

$$\omega(\mathbf{x}, t) \approx \omega^h(\mathbf{x}, t) = \sum_{i=1}^{N} \Gamma_i(t) \zeta_\sigma \left(\mathbf{x} - \mathbf{x}_i(t)\right), \tag{3}$$

where $\mathbf{x}_i$ is the particle position, Γ_i is its circulation, and the core size is σ. The characteristic distribution of vorticity ζ_σ (commonly called the cutoff function) is a Gaussian: $\zeta_\sigma(\mathbf{x}) = 1/(2\pi\sigma^2) \exp\left(-|\mathbf{x}|^2/2\sigma^2\right)$.

The vorticity–velocity formulation is complete after obtaining the velocity at each point (each particle location) using the Biot–Savart law, which in 2D is expressed by:

$$\mathbf{u}(\mathbf{x},t) = \frac{-1}{2\pi}\int \frac{(\mathbf{x}-\mathbf{x}')\times\omega(\mathbf{x}',t)\hat{\mathbf{k}}}{|\mathbf{x}-\mathbf{x}'|^2}d\mathbf{x}'. \tag{4}$$

The numerical method is implemented by integrating the particle trajectories using the velocity obtained from (4), and incorporating the effects of viscosity by changing the local distribution of vorticity of each particle. The most prevalent viscous method applies a change to the circulation strength (called particle strength exchange, or PSE method), but we use an alternative method which applies the change to the particle radius. It is named core spreading method, and it satisfies the diffusion equation at each particle exactly by growing σ^2 linearly according to $d\sigma^2/dt = 2\nu$. To maintain the accuracy of discretization over a time marching calculation, a spatial adaptation scheme is applied. It is based on radial basis function interpolation of the vorticity field, to obtain a new, well-overlapped particle set every few time steps. The core sizes are also reset at this stage to ensure a convergent core spreading vortex method. The method is described in detail in [2].

2.2. Finding the Lagrangian geometry

Figure 1 shows that the flow is essentially time dependent; therefore the relation between particle trajectories and the geometry of the instantaneous velocity field is not straightforward. We expect, however, that if a saddle point exists long enough and the velocity field around it changes slowly then a hyperbolic particle will exist in its neighborhood. This condition is satisfied uninterruptedly in all cases studied here, therefore the hyperbolic particle and its manifolds at any given time t can be computed by the method described below. With suitable variations, this method has been extensively used for velocity fields defined analytically or given as data sets, and with periodic, quasi-periodic or arbitrary time dependence [3, 8, 12, 16].

The first step is to compute Ψ, the stream function observed in a system where the flow is approximately steady. This is given by the simple transformation $\Psi = \psi + \frac{1}{2}\Omega\left[(x-x_c)^2 + (y-y_c)^2\right]$, where ψ is the stream function obtained by the numerical calculation, Ω is the approximate angular velocity of the vortex and (x_c, y_c) is its center of rotation. Because of the initial symmetry, the vortex center is also the center of rotation, so we only need to determine the value of Ω. The value chosen is the one that minimizes the Jacobian $J(\Psi,\omega)$. Note that other methods are available but they give slightly different results [6, 10, 13].

The second step is to determine the geometry of the (approximately) corotating stream function Ψ; that is to say, locate the saddle stagnation points and the streamlines associated to them (see [16] for the method used here).

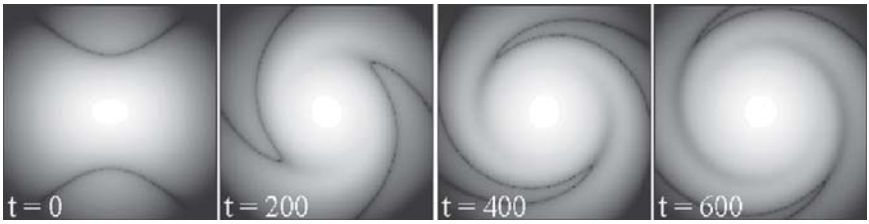

(a) $\delta = 0.1$

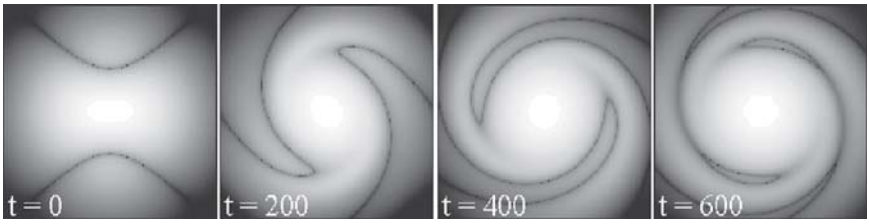

(b) $\delta = 0.175$

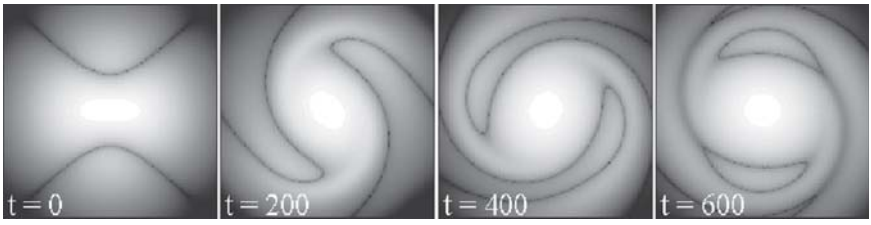

(c) $\delta = 0.25$

Fig. 1. Plots of logarithm of $|\omega|$ for different amplitudes of perturbation at Reynolds number $Re = 3000$.

Finally, the stable manifold is obtained by computing the evolution, from time $t + \Delta t$ to time t, of a short line which crosses the saddle point of $\Psi(x, y, t + \Delta t)$ in the attracting direction; and the unstable manifold is obtained computing the evolution, from time $t - \Delta t$ to time t, of a short line which crosses the saddle point of $\Psi(x, y, t - \Delta t)$ in the repelling direction. The position of the hyperbolic particle is given by the intersection of the manifolds.

3. Numerical Results

We present results for several combinations of parameters, for which we have calculated the evolution of the vorticity field and have obtained the flow geometry, using the methods described in the previous section.

For a given Reynolds number, as the amplitude of the initial quadrupolar perturbation, δ, is increased the flow evolves in the following ways. For small δ, the perturbation winds-up and decays and the flow quickly axisymmetrizes.

There is next a range of values of δ for which the flow seems to form a "transient tripole", in which weak satellites of negative vorticity only survive for a short time and decay due to diffusion. For larger values of δ, the tripole is able to reach a quasi-steady state, still decaying by diffusion, but surviving for several turnover periods. To illustrate these three "regimes", Fig. 1 shows plots in grey-scale of the logarithm of $|\omega|$ for three different runs with $Re = 3000$; the dark line indicates where the vorticity changes sign.

For the first case in Fig. 1, the negative vorticity inclusions are quickly stretched and "squeezed" inside the zero-vorticity contour; the negative perturbation is expelled to larger radii, and the flow axisymmetrizes. In the middle case, the zero-vorticity contour pinches as it spirals, isolating momentarily two small inclusions of negative vorticity (see Fig. 1(b), $t = 600$). These inclusions are so small and weak that they disappear by $t = 700$ and the flow proceeds to axisymmetrize. For the larger value of δ, the isolated negative inclusions are larger and stronger, and hence the tripole reaches a quasi-steady state, decaying slowly; the satellites in this case survive until $t = 1500$.

A good diagnostic to reveal that the flow has reached a steady-state is the scatter plot of (ω, ψ). For steady, inviscid flows, the Jacobian $J(\psi, \Delta\psi) = 0$, which implies the existence of some functional relation between streamfunction and vorticity. In any rotating frame of reference, a scatter plot is obtained by simply plotting the value of vorticity *versus* that of the streamfunction on the points of a sampling grid. A functional relation is indicated by very little scatter of the points, implying that the tripole is close to stationary in that frame of reference. As shown in Fig. 2, at $t = 800$ after the tripole is formed, the flow is close to steady (right-most plot) for both cases shown.

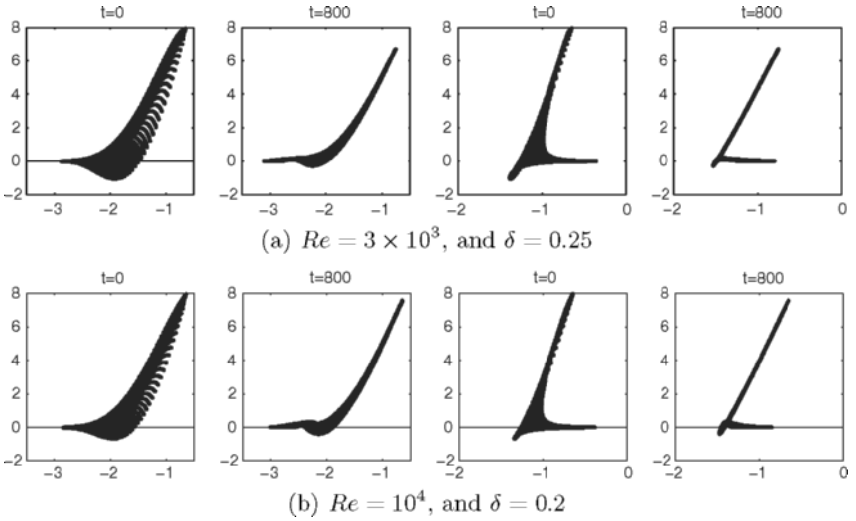

Fig. 2. (ω, ψ) scatter plots for tripoles with different parameters. Two left columns: uncorrected ψ; two right columns: ψ corrected for the tripole rotation. At $t = 800$, the structure is quasi-steady.

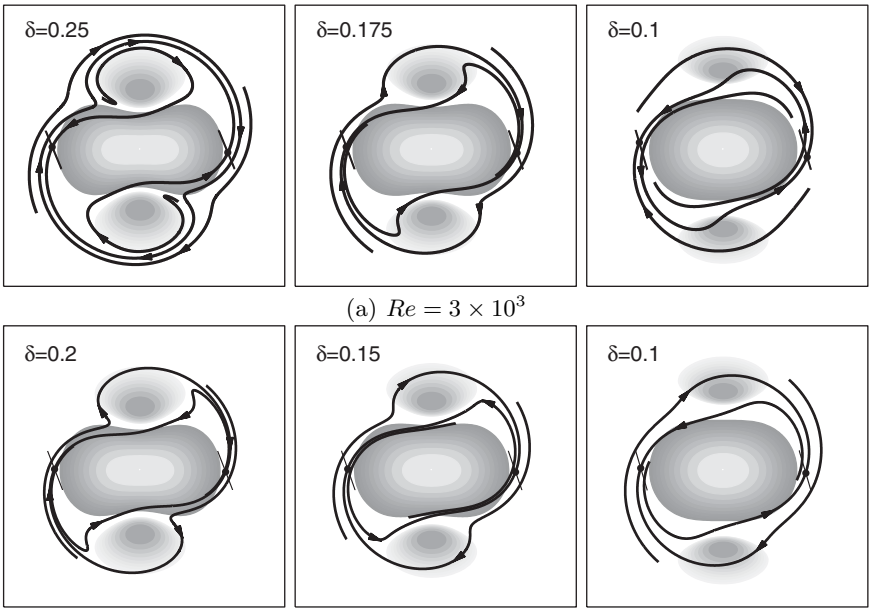

Fig. 3. Stable manifolds of the hyperbolic trajectories for three different amplitudes of the initial perturbation. A quasi steady tripole is formed for the case with larger amplitude, whereas for the smaller amplitudes the flow axisymmetrizes. For the mid-value of amplitude, small transitory satellites are formed and then quickly disappear.

The scatter plots in Fig. 2 are shown for the uncorrected (two left columns) and corrected streamfunction (two right columns). As mentioned before, the vortex continuously changes its shape while rotating with a variable angular speed. Thus, the rotating frame for the corrected streamfunction is chosen so that the Jacobian $J(\psi, \Delta\psi)$ is minimized, and thus it is the frame in which the structure is closest to steady, at any given time. As mentioned before, there are other choices of rotating frame.

The plots in Figs. 3(a) and 3(b) show the vorticity in logarithmic contours on a grey scale, and the stable manifolds at the initial time, for various runs. The arrows point in the direction of the flow on the manifold, and the black dot indicates the position of the hyperbolic trajectory. For all different values of δ and Re shown, most of the vorticity in the satellites lies between the two manifolds. However, only in the left-most cases, with the larger values of δ, does a tripole form. In these two cases, the tripole reaches a quasi-steady state, which can be confirmed from the scatter plot, Fig. 2(b), where the (ω, ψ) points show little scatter at $t = 800$.

We now present the evolution of the flow geometry for two cases that develop a tripole, with different Reynolds number. Fig. 4(a) corresponds to $Re = 3000$, and Fig. 4(b) to $Re = 10^4$. The stable and unstable manifolds are

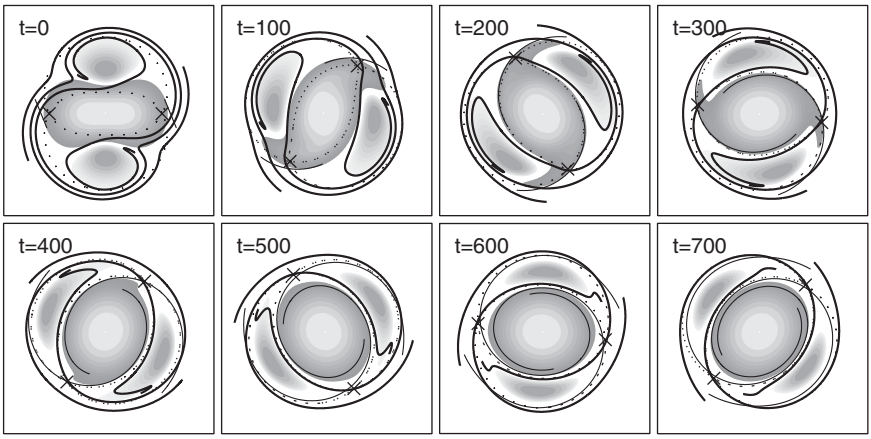

(a) $Re = 3 \times 10^3$, and $\delta = 0.25$

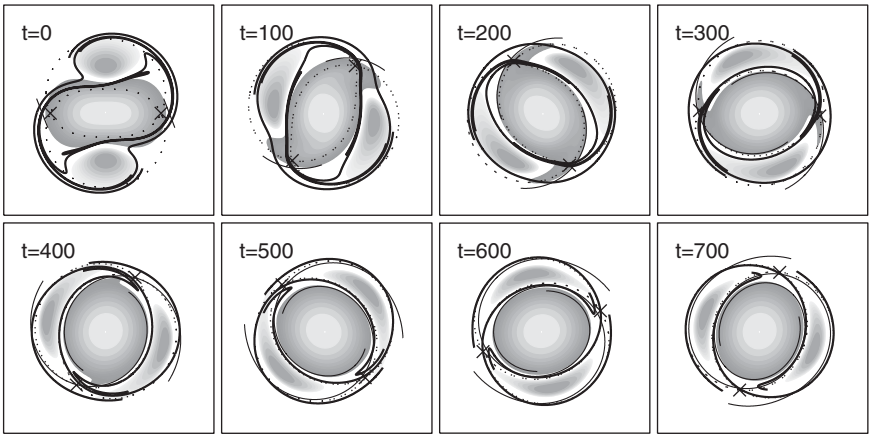

(b) $Re = 10^4$, and $\delta = 0.2$

Fig. 4. Stable and unstable manifolds (thick and thin lines, respectively) and Eulerian separatrices (dotted) for the time-evolving tripole with different parameters.

shown for different time slices; the Eulerian representation of the flow geometry — given by the separatrices in a frame rotating with the instantaneous angular velocity — is shown in dotted lines.

Irrespective of the amplitude of the perturbation, the Eulerian flow geometry has the same topology: three stagnation points of centre type, two saddle points, and the corresponding separatrices. Therefore, the Eulerian flow geometry does not distinguish whether the vortex will develop into a tripolar or a monopolar vortex. In conclusion, it is not correct to ascribe the persistence of the satellites in the tripole to the formation of a critical separatrix, as suggested before [13].

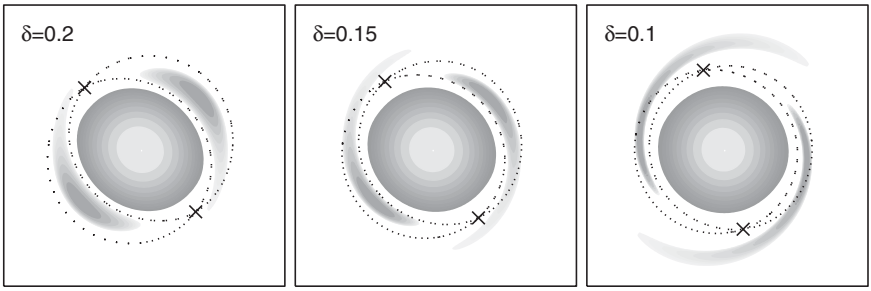

Fig. 5. Eulerian geometry at $t = 500$ for three cases with $Re = 10^4$.

The non-distinguishing nature of the Eulerian geometry is also seen in Fig. 5, which shows the separatrices at a time $t = 500$ for three cases with $Re = 10^4$. Irrespective of the amplitude of the perturbation, the topology of the co-rotating streamfunction is the same, with three centres and one saddle stagnation point. The difference for a case leading to a tripole can only be seen in the Lagrangian geometry, where the hyperbolic trajectories exist for the whole evolution.

4. Conclusion

We have obtained the Lagrangian flow geometry for several cases of non-shielded tripole evolution. The non-shielded tripole is characterized by a critical level of the non-axisymmetric component in the initial condition below which the flow evolves to axisymmetry, and above which a quasi-steady tripole is obtained. The existence of such a threshold had been previously ascribed to the appearance of a critical separatrix in the co-rotating streamfunction. By obtaining and comparing the Eulerian and Lagrangian geometries of the flow, we find that the Eulerian separatrices cannot distinguish between a tripole and a mildly perturbed monopole leading to axisymmetrization. Only in the Lagrangian features of the flow can a distinction be found, where for the tripole hyperbolic trajectories are present during the whole evolution.

Acknowledgements

Computing time provided by the Laboratory for Advanced Computation in the Mathematical Sciences, University of Bristol (`http://lacms.maths.bris.ac.uk/`). Thanks to G.J.F. van Heijst for helpful discussions. LAB's travel made possible by a grant from the Nuffield Foundation.

References

1. L. A. Barba and A. Leonard. Emergence and evolution of tripole vortices from net-circulation initial conditions. *Phys. Fluids*, 19(1):017101, 2007.
2. L. A. Barba, A. Leonard, and C. B. Allen. Vortex method with meshless spatial adaption for accurate simulation of viscous, unsteady vortical flows. *Int. J. Num. Meth. Fluids*, 47(8–9):841–848, 2005.
3. D. Beigie, A. Leonard, and S. Wiggins. Invariant manifold templates for chaotic advection. *Chaos, Solitons & Fractals*, 4:749–868, 1994.
4. X. J. Carton, G. R. Flierl, and L. M. Polvani. The generation of tripoles from unstable axisymmetric isolated vortex structures. *Europhys. Lett.*, 9:339–344, 1989.
5. C. Cerretelli and C. H. K. Williamson. The physical mechanism for vortex merging. *J. Fluid Mech.*, 475:41–77, 2003.
6. D. G. Dritschel. A general theory for two-dimensional vortex interaction. *J. Fluid Mech.*, 293:269–303, 1995.
7. J. B. Flor, W. S. S. Govers, G. J. F. van Heijst, and R. Van Sluis. Formation of a tripolar vortex in a stratified fluid. *Applied Sci. Res.*, 51:405–409, 1993.
8. N. Malhotra and S. Wiggins. Geometric structures, lobe dynamics, and Lagrangian transport in flows with aperiodic time-dependence with applications to Rossby wave flow. *Journal of Nonlinear Science*, 8:401–456, 1998.
9. M. V. Melander, J. C. McWilliams, and N. J. Zabusky. Axisymmetrization and vorticity-gradient intensification of an isolated two-dimensional vortex through filamentation. *J. Fluid Mech.*, 178:137–159, 1987.
10. M. V. Melander, N. J. Zabusky, and J. C. McWilliams. Symmetric vortex merger in two dimensions: causes and conditions. *J. Fluid Mech.*, 195:303–340, 1988.
11. P. Orlandi and G. J. F. van Heijst. Numerical simulation of tripolar vortices in 2D flow. *Fluid Dyn. Res.*, 9:179–206, 1992.
12. V. Rom-Kedar, A. Leonard, and S. Wiggins. An analytical study of transport, mixing and chaos in an unsteady vortical flow. *Journal of Fluid Mechanics*, 214:347–394, 1990.
13. L. F. Rossi, J. F. Lingevitch, and A. J. Bernoff. Quasi-steady monopole and tripole attractors for relaxing vortices. *Phys. Fluids*, 9:2329–2338, 1997.
14. G. J. F. van Heijst and R. C. Kloosterziel. Tripolar vortices in a rotating fluid. *Nature*, 338:569–571, 1989.
15. G. J. F. van Heijst, R. C. Kloosterziel, and C. W. M. Williams. Laboratory experiments on the tripolar vortex in a rotating fluid. *J. Fluid Mech.*, 225:301–331, 1991.
16. O. U. Velasco Fuentes. Chaotic advection by two interacting finite-area vortices. *Phys. Fluids*, 13(4):901–912, 2001.
17. O. U. Velasco Fuentes. Vortex filamentation: its onset and its role on axisymmetrization and merger. *Dyn. Atmos. Oceans*, 40:23–42, 2005.